Chalcogenide Letters Vol. 22, No. 2, February 2025, p. 97 - 108

Fabrication and characterization of Cu (In, Ga) Se_2 thin films by electrodeposition: optimization of the thermal treatment with selenium and mechanical disturbance technique

A. Ledesma-Juárez [a], J. F. Quintero-Guerrero [b], A. M. Fernández [a,*]
[a] *Renewable Energy Institute, National Autonomous University of Mexico, Av. Xochicalco S/N, Temixco, Morelos, 62580, México*
[b] *Center for Research in Engineering and Applied Sciences, Autonomous University of the State of Morelos Av. Universidad No 1001, 62209, Cuernavaca, Morelos. México*

The evaporation technique fabricates solar cells using the Cu(In, Ga)Se_2 (CIGS) absorber. This technique has strong limitations in preparing this absorber in a large area, necessitating the electrodeposition technique. However, the morphology and crystallinity of this absorber need to be sufficiently adequate to guarantee proper collection of charge carriers since a cauliflower-type growth is favored. This underscores the need for modifications during the synthesis, thermal treatments, and post-synthesis to improve the morphology and crystallinity, a complex and significant aspect of our research. This work discusses the structural, atomic composition, morphological, and optical results obtained for samples of CIGS films synthesized by the electrodeposition technique. We proudly report that we achieved the best atomic composition, close to the ideal and an adequate morphology, by selenizing the samples with 30 mg and a temperature of 570°C. This success was further enhanced by subjecting these films to constant periodic movement during their synthesis, leading to significant improvements in the crystallinity, a testament to the success of our research.

(Received September 11, 2024; Accepted February 1, 2025)

Keywords: CIGS, Electrodeposition, Selenizaion

1. Introduction

Cu(In, Ga)Se_2 (CIGS) thin films, a highly promising option for thin-film solar cell production, are uniquely fabricated by electrodeposition. This technique offers numerous advantages over alternative methods, such as vacuum use, including large-area deposits, efficient material utilization, lower energy consumption during absorber growth, element optimization, and low manufacturing cost. These advantages make a compelling case for the widespread adoption of the electrodeposition technique in materials science and solar cell production.

Due to the low crystallinity of the CIGS films (Copper, Indium, Gallium, and Selenium) manufactured by electrodeposition, [3] the selenization process becomes a crucial step. It ensures the recrystallization of the absorber material and promotes grain growth, thereby significantly improving the properties of the CIGS films. [4]

The selenization process plays an important role in the fabrication of CIGS films manufactured by electrodeposition because it promotes the change of the chemical and crystalline structure of the CIGS film, improving the electrical and optical properties of the material; it allows proper integration of selenium into the CIGS structure; it can help to reduce the presence of defects in the film, such as surface defects. [5,6]

For these reasons, it is essential to have control of this process to ensure consistent and reproducible results. Applying mechanical perturbations can affect the nucleation and growth of crystals during deposition. Likewise, they can help eliminate crystalline defects, such as dislocations

* Corresponding author: afm@ier.unam.mx
https://doi.org/10.15251/CL.2025.222.97

and grain boundaries, improve the adhesion of the CIGS film to the substrate, and influence the film's morphology and thickness. [7,8]

This work uses a series of selenization tests on CIGS films fabricated by the electrodeposition technique using a system developed and constructed in the laboratory. The temperature and the amount of selenium used were varied, and mechanical perturbations were applied to some samples during the growth of the absorber. The objective was to find a suitable recrystallization process and to validate the importance of using such perturbations. As a result of these tests, the bandwidth values of the samples improved, obtaining results close to those reported in the literature for this material.

2. Experimental

2.1. Fabrication of CIGS films

The chemical composition of the electrolytic bath used to synthesize the CIGS thin films was 2.6 mM $CuCl_2$ chloride (99.99 %), 4.5 mM $InCl_3$ (99.99 %), 10 mM $GaCl_3$ (99.99 %), 8 mM H_2SeO_3, and one mM LiCl (99 %). All the reagents were from Sigma Aldrich. The reagents were dissolved in a buffer solution of pH 3, and the pH was adjusted with HCl (37.4 % vol).

Molybdenum (Mo) on Soda Lime Glass (SLD) as a substrate. The Mo had prepared in-house using direct current sputtering equipment, model Balzer BAE 250, with a Mo target of 5.08 cm.

The CIGS films were fabricated by co-electrodeposition [9] using the reagents and molarity listed in Table 1. They made them using a potentiostat/galvanostat model 263A, CorrWare software, and the chronoamperometry technique. The deposition time was one hour, and the voltage was -1.0V. Part of these films were obtained by mechanically perturbating the working electrode, every 15 minutes during the deposition time. The mechanical disturbance technique consists of moving the working electrode at constant time intervals to enhance the growth of the CIGS thin film. Its purpose is to provoke the formation of CIGS nuclei in different regions of the substrate, which allows for a homogeneous covering. For this reason, two types of CGIS films were obtained: the perturbed and the unperturbed ones.

2.2. Selenization of CIGS films

The experimental conditions applied to the CIGS films to trigger the recrystallization process were heat treatment at various temperatures and with different amounts of selenium. Table 1 shows the experimental conditions for each sample. Figure 1 shows a schematic of the components of the equipment. The equipment, a crucial part of our research, consists of a vacuum chamber and an oven (temperature source), which provides uniform heating over the film surface; selenium (99.99%) acquired from Sigma Aldrich was used. We used a nitrogen atmosphere during the process to prevent oxidation of the films. The following conditions were used: initial pressure of 1.9 x 10-5 hPa, pressure during the process was 2.2 x 10-2 hPa during one hour.

The CIGS films MC1-A, MC1-B, and MC1-C were recrystallized at 550, 560, and 570°C with a carefully measured 30 mg selenium, ensuring the utmost precision in our experimental process.

CIGS films MC1-CS1, MC1-CS2, MC1-CS3, and MC1-CS4 were recrystallized at 570°C using 3, 15, 60 and 300 mg selenium.

Considering the two types of films obtained, which we refer to as 'perturbed' and 'not perturbed, 'the samples underwent recrystallization. The 'not perturbed' ones were recrystallized at 570°C, with the following amounts of selenium 3, 15, 60, and 300 mg forming the samples MC1-CS1, MC1-CS2, MC1-CS3, and MC1-CS4, respectively. The 'perturbed' ones, also recrystallized at 570°C, using 3, 15, 30, 60, and 300 mg of selenium, afforded the following CIGS samples MC1-CS1P, MC1-CS2P, MC1-CP, MC1-CS3P, and MC1-CS4P respectively.

Table 1. Description of the experimental conditions for each sample.

Sample number	Experimental conditions
Preparation with Temperature variation	
MC1	Unselenized
MC1-A	sample heat-treated at 550 °C with 30 mg of selenium
MC1-B	sample heat-treated at 560 °C with 30 mg of selenium
MC1-C	sample heat-treated at 570 °C with 30 mg of selenium
Preparation with selenium variation	
MC1-CS1	sample heat-treated at 570 °C with 5 mg of selenium
MC1-CS2	sample heat-treated at 570 °C with 15 mg of selenium
MC1-CS3	sample heat-treated at 570 °C with 60 mg of selenium
MC1-CS4	sample heat-treated at 570 °C with 300 mg of selenium
Prepared with mechanical perturbation, denoted by adding the letter 'P' in the nomenclature	
MC1-CS1P	sample heat-treated at 570 °C with 5 mg of selenium and mechanical disturbance
MC1-CS2P	sample heat-treated at 570 °C with 15 mg of selenium and mechanical disturbance
MC1-CP	sample heat-treated at 570 °C with 30 mg of selenium and mechanical disturbance
MC1-CS3P	sample heat-treated at 570 °C with 60 mg of selenium and mechanical disturbance
MC1-CS4P	sample heat-treated at 570 °C with 300 mg of selenium and mechanical disturbance

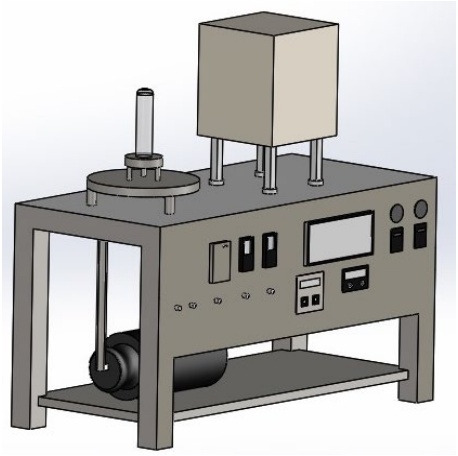

Fig. 1. Schematic representation of the selenization chamber.

2.3. Characterization

DMAX-2200 X-ray diffraction equipment obtained patterns of each film with copper Kα radiation (λCu = 1.5406 Å). The X-ray beam had a grazing incidence of 0.5° (GIXRD).

The morphology of the films and their atomic composition using the EDS technique were comprehensively obtained using the versatile Hitachi SEM Microscope model S-5500 with a secondary electron detector and an energy-dispersive X-ray detector model INCA-x-act. An electron accelerating voltage of 20 kV and energy emission levels Kα for copper, selenium, gallium, and Lα for indium were used to quantify the atomic composition.

The atomic composition was also measured by inductively coupled plasma atomic emission spectroscopy (ICP-AES) using the Horiba Ultima 2 spectrometer. The equipment was meticulously calibrated with a solution containing Cu, In, Ga, and Se, ensuring the utmost accuracy in our measurements. The emission lines 327,369, 230,606, 417, 206, and 196,026 nm for Cu, In, Ga, and Se were used for quantification, respectively.

The thicknesses of the films were measured using the Alpha-step 100 profilometer.

A Jasco V-670 UV-visible spectrophotometer was used to record the diffuse reflectance spectra within the 2500 to 250 nm wavelength range. The band gap of the films was obtained using the Kubelka-Munk equation.

The Kubelka-Munk equation [10, 11] can be written at any wavelength as in equation (1):

$$\frac{K}{S} = \frac{(1-R_\infty)^2}{2R_\infty} = F(R_\infty) \tag{1}$$

R∞ is the diffuse reflectance, and F(R∞) is called the Kubelka-Munk function. The absorption coefficient and band structure Eg were related through the well-known Tauc relation, given by the expression for a direct bandgap material.

$$\alpha h\upsilon = A\left(h\upsilon - E_g\right)^n \tag{2}$$

where α is the linear absorption coefficient, υ is the light frequency, and A is the proportionality constant. The value of n is equal to 1/2 for direct bandgap materials. When the incident radiation scatters in a perfectly diffuse manner, the absorption coefficient K is equal to 2α. In this case, the Kubelka- Munk function is proportional to the absorption coefficient α, we obtain the relation:

$$[F(R_\infty)h\upsilon]^2 = (ah\upsilon)^2 \tag{3}$$

3. Results and discussion

3.1. Structural analysis by XRD

Figure 2 shows the diffractograms of the CIGS films, (a) unselenized, (b) selenide at different Temperatures (550, 560, and 570 °C), selenide with 30 mg selenium, (c) and selenide using different amounts of selenium (3, 15, 30, 30, 60 and 300 mg) and baked at 570°C, (d) selenide and mechanically perturbed during the adsorber growth process, using different amounts of selenium (3, 15, 15, 30, 60 and 300 mg) and baked at 570°C.

Figure 2 (a) shows the diffractogram of the CIGS film obtained without selenization treatment. It exhibits an amorphous behavior with no diffraction peaks. In contrast, Figures 2 (b), (c), and (d) show peaks of the CuGa0.3In0.7Se2 (PDF 35-1102) and Mo (PDF 42-1120) phases, with the planes (112), (110), (220) and (116). Phases showing the highest intensity. The MC1-C and MC1-CP samples show larger and more defined peaks, indicating the presence of larger crystals, as confirmed by SEM micrographs (Figure 3). A more ordered crystal structure can lead to a higher mobility of charge carriers, which can enhance the photovoltaic response, making it a crucial factor in the performance of CIGS films.

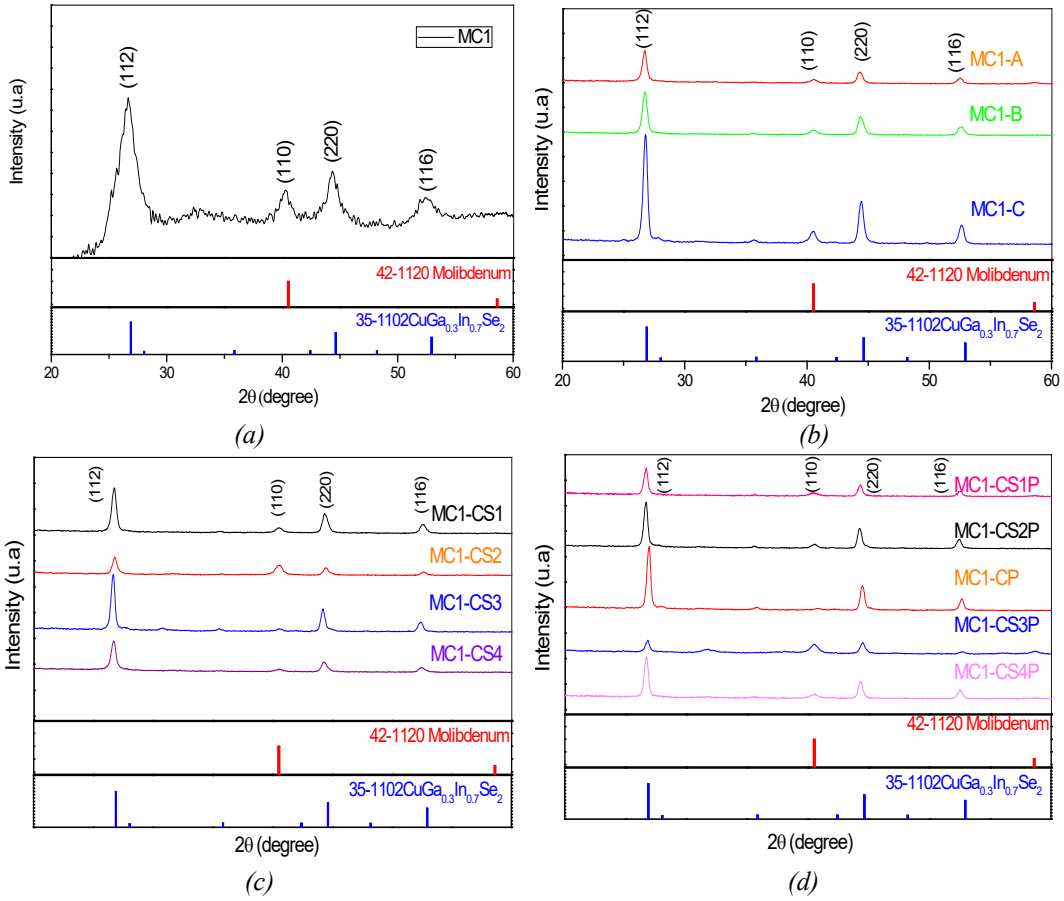

Fig. 2. X-ray diffraction spectra of CIGS films, (a) un-selenide, (b) selenide by varying the temperature (550, 560, and 570°C) using 30 mg of selenium, (c) selenide by varying the amount of selenium (3, 15, 60, 300 mg) using a temperature of 570°C and (d) using mechanical perturbations during absorber growth and selenide by varying the amount of selenium (3, 15, 30, 60, 300 mg) at 570°C.

3.2. Atomic composition analysis by ICP-AES

The atomic percentage values and film thicknesses are in Table 2. Considering that the ideal Cu/(In+Ga) and Ga/(In+Ga) atomic ratios have values of 0.9 and 0.3, respectively, it is possible to observe that for sample MC1, these values are far apart. Increasing the MC1 temperature According to the values shown in Table 2 of the atomic ratios for the MC1 sample, without any heat treatment nor subjected to mechanical disturbances, during its synthesis, observed that the values are far from the ideal or suggested ratios to obtain an absorber film and use in the construction of a solar cell. When increasing the temperature during the treatment, from 550°, 560°, and 570°, with 30 mg of selenium, observed that these ratios are getting closer to the ideal values, as can be observed for samples MC1-A, MC1-B, and MC1-C. From these values, it is possible to affirm that the sample baked at 570°C, in Se, has values closer to the ideal values, as can be seen with the values of sample MC1-C. Using different amounts of Se (3,15,60 and 300 mg) of sample MC1 and heated at 570°C, obtained samples MC1-CS1, MC1-CS2, MC1-CS3, and MC1-CS4, respectively, whose values of atomic ratio composition are in the table. It can be seen from the table that none of the values are close to those obtained when baked at 30 mg Se and 570°C.

Table 2. Percentage values of the atomic composition obtained by ICP-AES and thicknesses of the CIGS fabricated films.

Sample	Atomic values (% At.)						Thickness (μm)
	Cu	**In**	**Ga**	**Se**	**Cu/(In+Ga)**	**Ga/(In+Ga)**	
Using different temperatures							
MC1	23.47	17.12	3.18	56.20	1.16	0.15	1.1
MC1-A	43.16	16.38	6.91	33.53	1.85	0.29	1.0
MC1-B	34.80	15.71	7.40	42.08	1.50	0.32	1.2
MC1-C	30.98	27.47	9.06	32.47	*0.85*	*0.24*	*1.5*
Using different amounts of Selenium							
MC1-CS1	30.59	16.30	13.53	39.55	1.02	0.45	1.2
MC1-CS2	28.36	16.11	8.13	47.38	1.17	0.33	1.3
MC1-CS3	34.10	23.55	9.00	33.32	1.04	0.27	1.2
MC1-CS4	33.44	17.95	12.59	36.00	1.09	0.41	1.3
Using different amounts of Selenium and performing mechanical disturbance							
MC1-CP	33.16	25.73	8.87	32.23	0.95	0.25	1.4
MC1-CS1P	33.76	23.16	4.29	38.81	1.23	0.15	1.2
MC1-CS2P	32.33	19.72	5.73	42.21	1.27	0.22	1.1
MC1-CS3P	43.84	7.85	12.97	35.32	2.10	0.62	1.2
MC1-CS4P	37.70	22.36	6.64	33.28	1.30	0.22	1.2

When mechanical perturbations were applied during the preparation of the CIGS films and their subsequent heat treatment at 570°C in the presence of 3, 15, 30, 60, and 300 mg of Se, the samples MC1-CS1P, MC1-CS2P, MC1-CP, MC1-CS3P, and MC1-CS4P, respectively, were obtained.

The MC1-CP samples, with values closest to the ideal, point to practical implications. The best conditions for achieving ideal atomic composition involve subjecting the CIGS film to a mechanical disturbance treatment during its synthesis and then baking it at 570 °C with 30 mg of Se. This finding directly relates to constructing efficient solar cells, making our research theoretical and highly applicable to real-world scenarios.

3.3 Morphological analysis by SEM

Figure 3 shows the micrographs of the CIGS films obtained by SEM (1.00μm), amplified at 50 KX. Figure 3(a) shows the morphology of sample MC1, which does not have any treatment. As the temperature increased during the selenization process, samples MC1-A, MC1-B, and MC1- were obtained, which were heat treated at temperatures of 550 (Figure 3(b)), 560 (Figure 3(c)) and 570°C (Figure 3(d)), respectively, were crystal formation observed; these being larger and more noticeable in the MC1-C sample. In these samples, 30 mg of selenium was used for the selenization process. When using 3 mg of selenium, sample MC1-CS1 was obtained (Figure 3(e), where it is observed that the CIGS film was without crystals. As the amount of selenium increases (15, 60, and 300 mg), the formation of crystals is observed, as shown in Figures 3 (f), (g), (h), which correspond to the MC1-CS2, MC1-CS3, and MC1-CS4 films. In contrast, a cauliflower-type morphology is formed in Figure 3(h), probably due to excess selenium.

Figure 3 (i), (j), (k), (l), (m) shows the morphology of the CIGS films to which mechanical perturbations were subjected during their synthesis and corresponded to sample number MC1-CS1P,

MC1-CS2P, MC1-CP, MC1-CS3P, and MC1-CS34P, respectively. It can be observed that the morphology of sample MC1-CP shows a possible crystal growth. With the application of mechanical perturbations, a larger area is achieved by forming a morphology with more crystalline-type material, as can be seen when comparing Figures 3 (d) and Figure 3 (k), corresponding to the MC1-C samples without perturbation and MC1-CP perturbed.

Figure 3 (n) shows the cross-section of sample MC1, which corresponds to the unselected sample, which, when compared with the selenized sample (Figure 3(o)), sample MC1-C and with the selenized and perturbed sample, MC1-CP (Figure 3(p)), a compact morphology and without regions with voids is observed, that is to say, it is observed that the morphology obtained without selenization, whose formation is of the cauliflower type, where a great number of hollows are followed, in figures 3(o), (p), a compact morphology is obtained and with a better crystallinity, evidencing then that a recrystallization process was obtained.

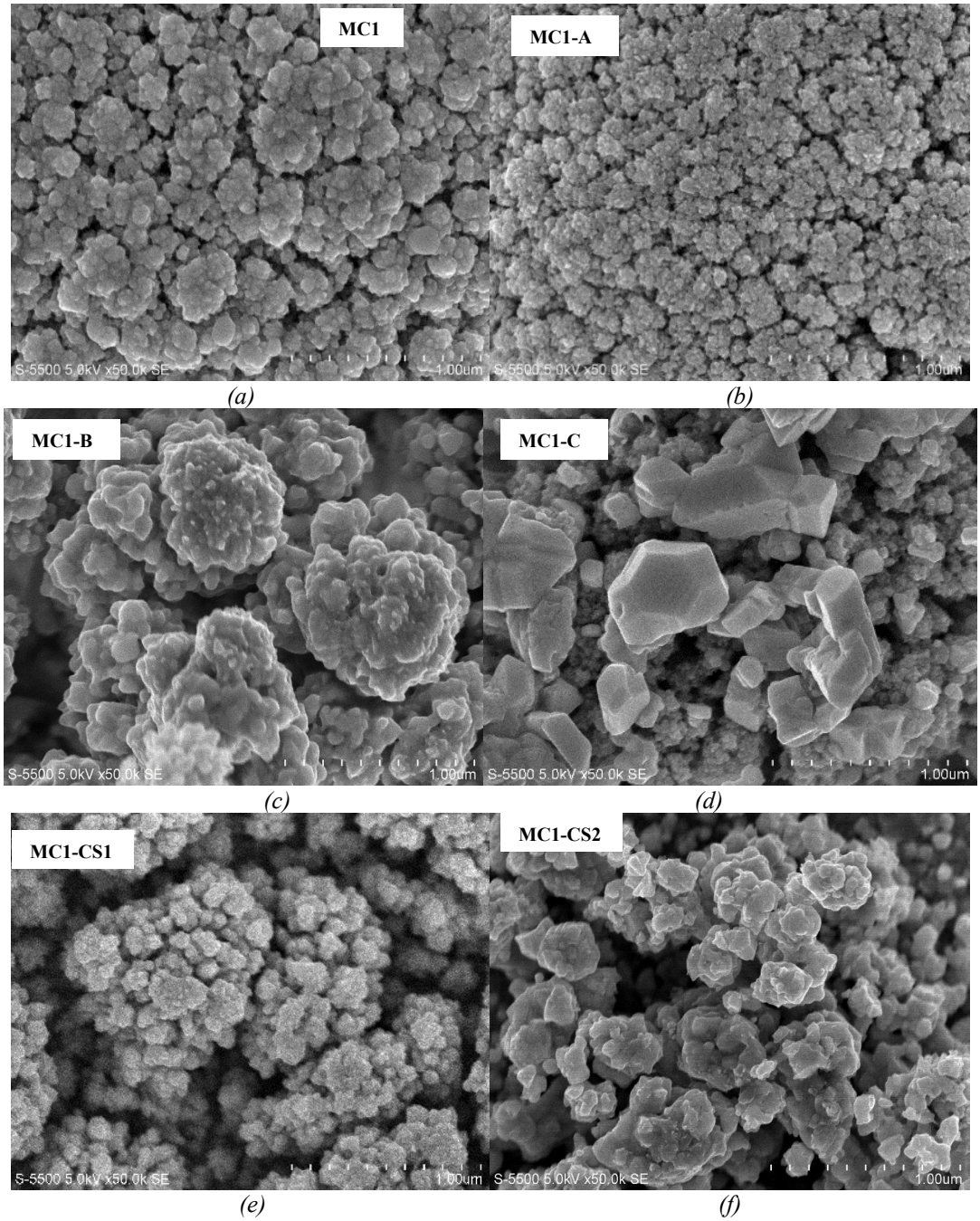

(a) *(b)*

(c) *(d)*

(e) *(f)*

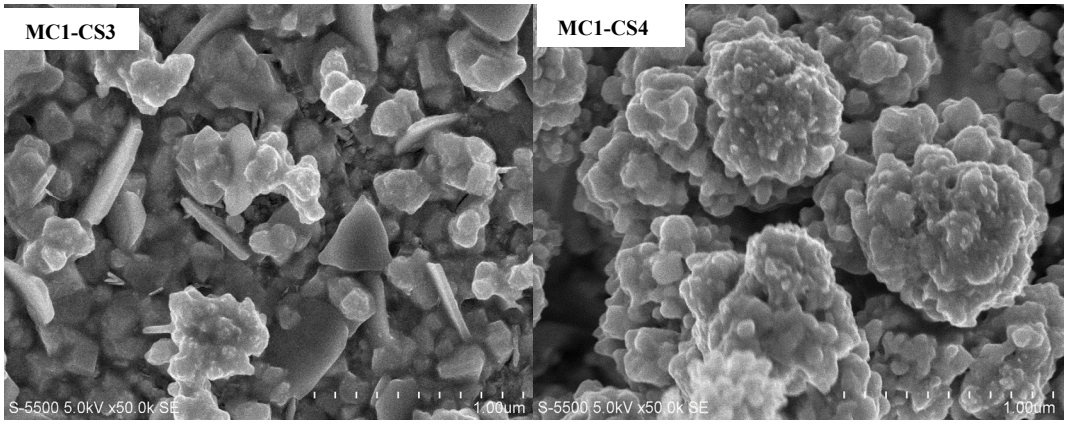
MC1-CS3
S-5500 5.0kV x50.0k SE
1.00um
MC1-CS4
S-5500 5.0kV x50.0k SE
1.00um

(g) *(h)*

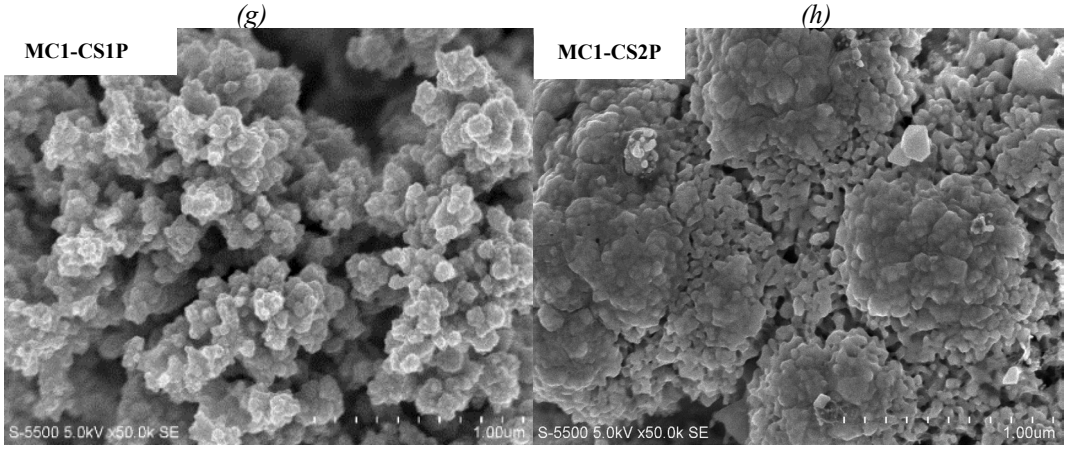
MC1-CS1P
S-5500 5.0kV x50.0k SE
1.00um
MC1-CS2P
S-5500 5.0kV x50.0k SE
1.00um

(i) *(j)*

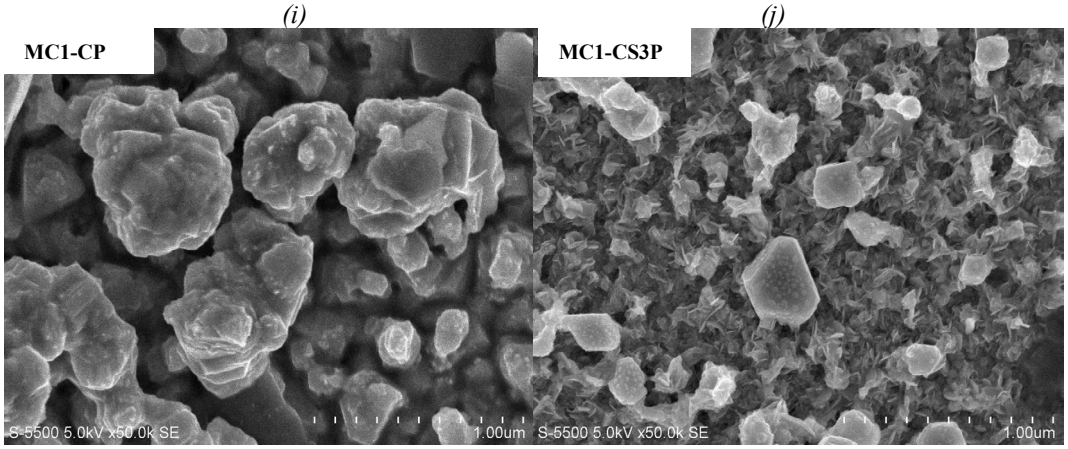
MC1-CP
S-5500 5.0kV x50.0k SE
1.00um
MC1-CS3P
S-5500 5.0kV x50.0k SE
1.00um

(l) *(k)*

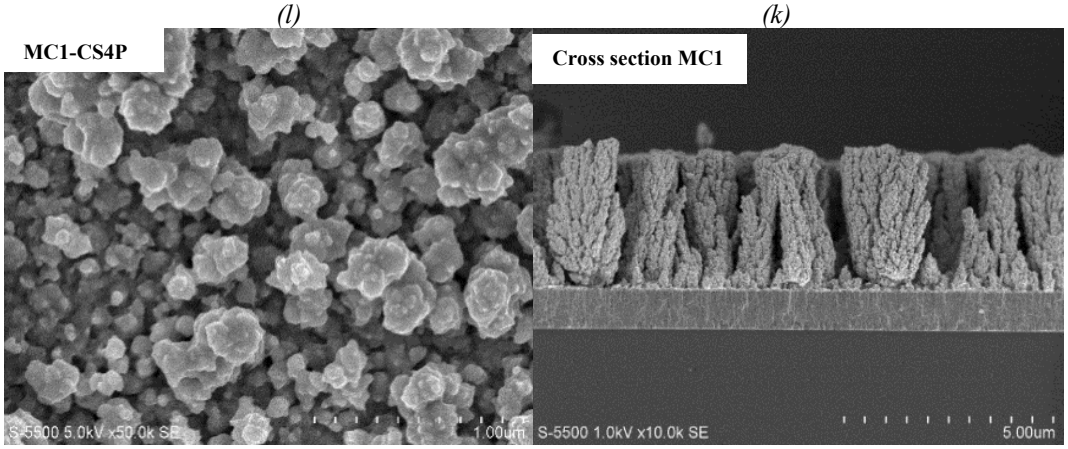
MC1-CS4P
S-5500 5.0kV x50.0k SE
1.00um
Cross section MC1
S-5500 1.0kV x10.0k SE
5.00um

(m) *(n)*

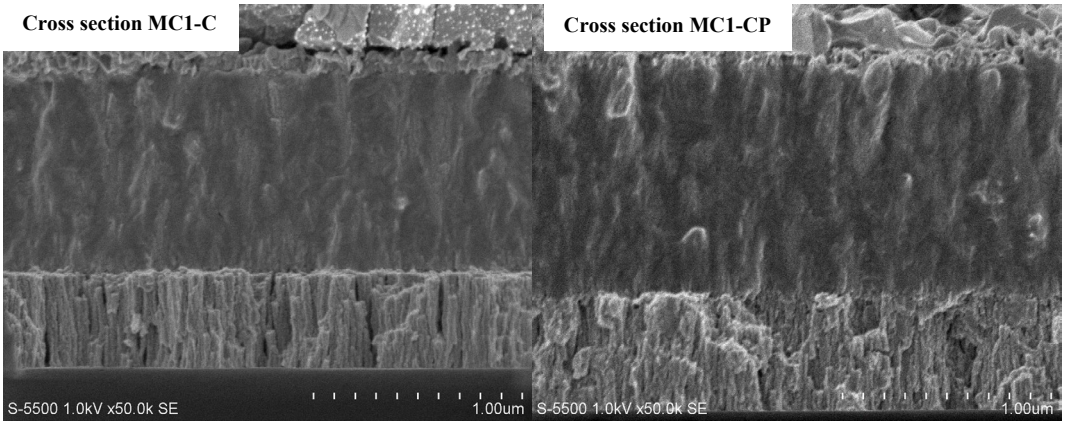

(o) *(p)*

Fig. 3. Micrographs of the CIGS films without applying mechanical perturbations and with mechanical perturbations, selenized under different conditions. (see sample description in section 3.3).

3.4. Optical properties

Figures 4 (a), (b), and (c) show the values of the diffuse reflectance for the CIGS films subjected to the selenization process at different amounts of selenium, treatment temperature, and subjected to perturbation during the formation of the thin films. Figures 5 (a), (b), and (c) show the plots of the Kubelka Munk function vs hv, which plot from the diffuse reflectance. From the latter plots, it is possible to calculate the film's bandwidth values in Table 3. In the samples treated at 550°, 560°, and 570°C, respectively, with 30 mg of selenium, the bandwidth values decreased (Figure 5(a)), which is possibly associated with a higher crystallinity as shown in Figures 5 (a), (b) and (c). By increasing the amount of selenium during heat treatment at a temperature of 570°C, the bandwidth values also tend to increase (Figure 5 (b)). However, no significant changes were observed, i.e., a cauliflower-type morphological structure still obtained, as observed in Figures 3(e), (f), (g), and (h). Where mechanical perturbations occur during the CIGS films' growth, the samples MC1-CS1P and MC1-CP (Figure 5 (c)) whose values are within the reported range. In contrast, the rest of the samples present a value higher than this (MC1- CS2P, -CS3P and -CS4P). Structural defects, such as vacancies or interstitial defects, can alter the material's electronic properties and affect the band gap size. [12].

Table 3. Band gap of selenized CIGS samples, varying Temperature (MC1-A, -B and -C), amount of selenium (MC1-CS1, CS2, -CS3 and -CS4), applying mechanical perturbations during absorber growth (MC1- CS1P, -CS2P, -CP, -CS3P and -CS4P.

Sample	Band gap value (eV)
MC1-A	2.0
MC1-B	1.9
MC1-C	1.8
MC1-CS1	1.7
MC1-CS2	1.6
MC1-CS3	1.7
MC1-CS4	2.4
MC1-CS1P	1.6
MC1-CS2P	2.0
MC1-CP	1.6
MC1-CS3P	2.0
MC1-CS4P	2.0

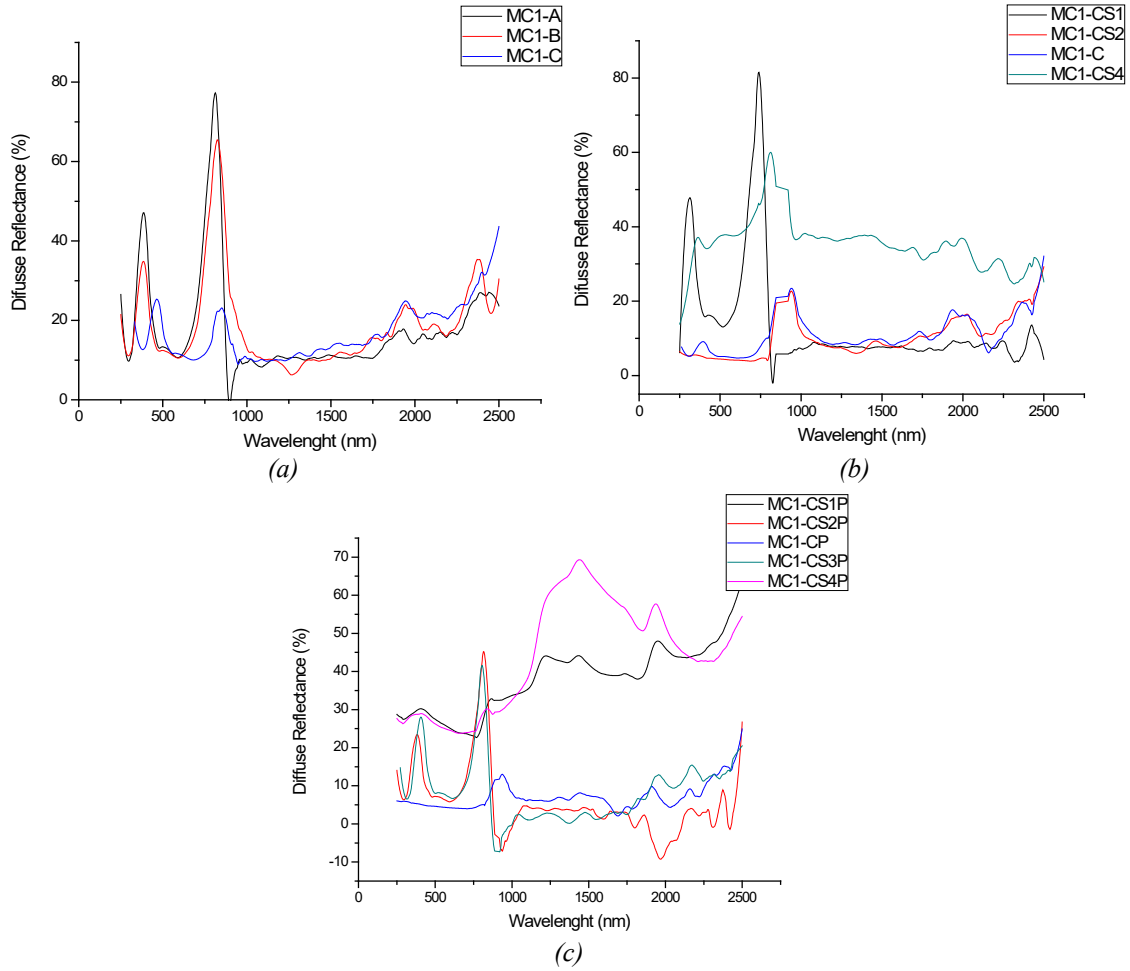

Fig. 3. Diffuse reflectance spectra of selenized CIGS films varying the (a) Temperature (550, 560 and 570°C, using 30mg selenium); (b) amount of selenium (3, 15, 60 and 300mg at 570°C); (c) varying the amount of selenium (3, 15, 30, 60 and 300 mg at 570°C) with the application of mechanical perturbations.

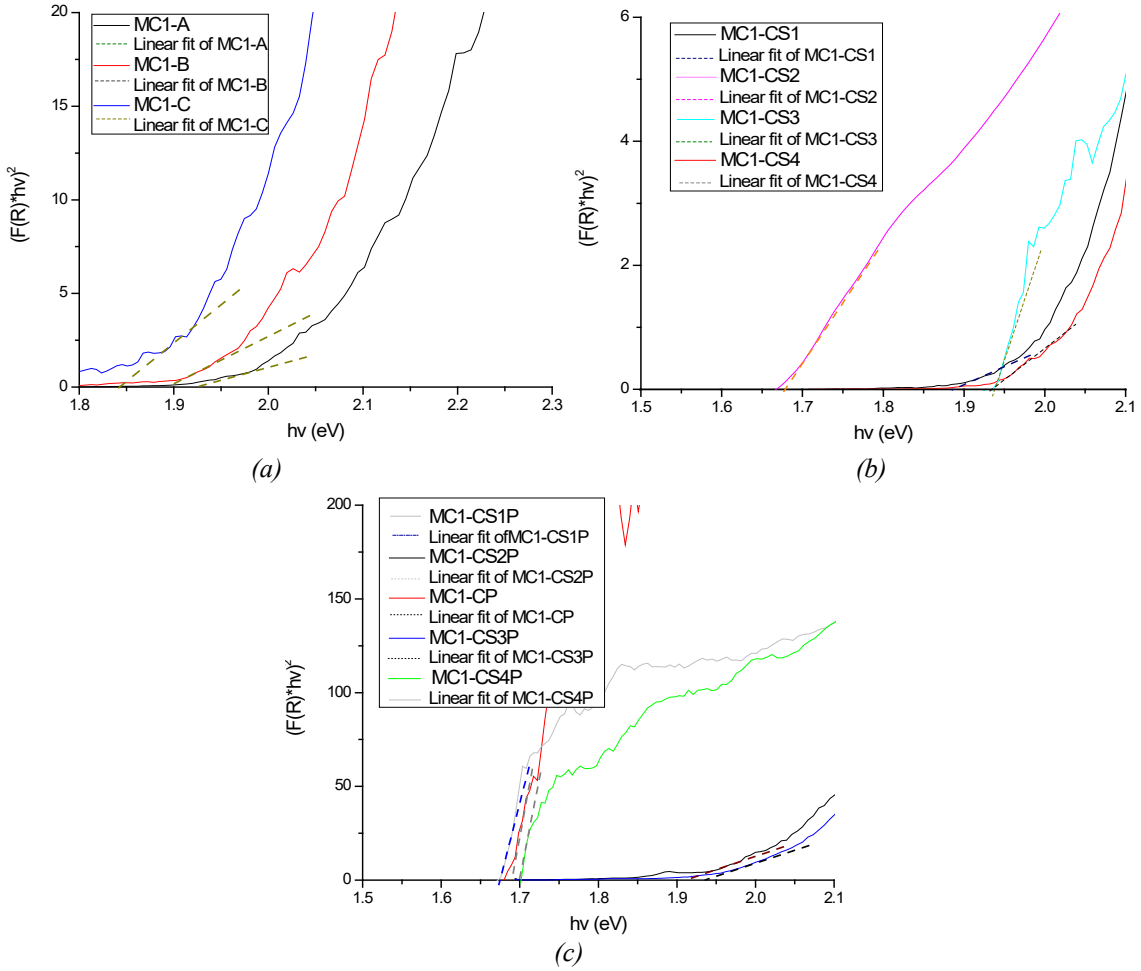

Fig. 4. Plots obtained by the Kubelka - Munk method for obtaining the band gap of CIGS films selenized by various methods varying the (a) temperature (550, 560 and 570°C, using 30 mg of selenium); (b) amount of selenium (3, 15, 60 and 300 mg at 570°C); (c) varying the amount of selenium (3, 15, 30, 60 and 300 mg at 570°C) with the application of mechanical perturbations.

4. Conclusion

Selenization is a crucial step in fabricating the CIGS absorber for application in solar cell development. As mentioned, the purpose is to improve the crystallinity of the CIGS layer. It changes the atomic composition and properties such as morphology and bandwidth, achieving this as was observed by subjecting the CGIS film to various temperatures in a selenium environment, at a temperature of 570°C, the change from a cauliflower-type morphology to a better crystallization of the grains.

On the other hand, when the selenization process occurred at different amounts of selenium, it was obtained that at 30 mg, the atomic composition and bandwidth values were substantially better than other amounts of selenium. Comparatively, samples of CIGS films were obtained by perturbation process and thermally treated with selenium observed that the crystallinity of the samples was improved. Applying mechanical perturbation during absorber growth may be a useful strategy to enhance the material properties and, ultimately, the efficiency of CIGS solar cells. Based on the results obtained from XRD, EDS, ICP-ES, SEM, and band gap, MC1-CP film applying mechanical perturbations during its deposition and selenized at 570°C, using 30mg selenium may be a good candidate as absorber material inside a thin film solar cell.

Acknowledgments

This work was supported through the PAPIIT IN115723. The authors would also like to thank CONAHCYT for their support under project CF-23-I1068. Arelis Ledesma-Juárez thanks CONAHCyT for the postdoctoral fellowship. We also thank Rogelio Morán Elvira for the SEM and EDS measurements and María Luisa Ramón García for the XRD measurements.

References

[1] Raghu N. Bhattacharya, Mi-Kyung Oh, Youngho Kim, Solar Energy Materials & Solar Cells, 98, 198 (2012); https://doi.org/10.1016/j.solmat.2011.10.026

[2] Jing-Yu Qu, Zheng-Fei Guo, Kun Pan, Wei-Wei Zhang, Xue-Jin Wang, Rare Metals, 36(9), 729 (2017); https://doi.org/10.1007/s12598-017-0941-6

[3] Raghu N. Bhattacharya, Solar Energy Materials & Solar Cells 113, 96 (2013); https://doi.org/10.1016/j.solmat.2013.01.028

[4] Sachin V. Desarada, Priyanka U. Londhe, Shweta Chaure, Nandu B. Chaure, Jornal of Materials Science: Materials in Electronics, 33, 203 (2022); https://doi.org/10.1007/s10854-021-07286-3

[5] Viswanathan S. Saji, Sang-Min Lee, Chi Woo Lee, Journal of the Korean Electrochemical Society, 14(2), 61 (2011); https://doi.org/10.5229/JKES.2011.14.2.061

[6] Roland Mainz, Alfons Weber, Humberto Rodriguez-Alvarez, Sergiu Levcenko, ManuelaKlaus, Paul Pistor, Reiner Klenk, Hans-Werner Schock, Progress in Photovoltaics: Research and Applications 23, 1131 (2014); https://doi.org/10.1002/pip.2531

[7] B. Lara-Lara, A. M. Fernández, Journal of Materials Science: Materials in Electronics 27, 5099 (2016); https://doi.org/10.1007/s10854-016-4400-1

[8] B. Lara-Laraa, A.M. Fernández, Superlattices and Microstructures 128, 144 (2019); https://doi.org/10.1016/j.spmi.2019.01.024

[9] Arelis Ledesma-Juárez, A. M. Fernández, Journal of Materials Science: Materials in Electronics, 34, 1461 (2023); https://doi.org/10.1007/s10854-023-10745-8

[10] M. Milosevic, S. L. Berets, Applied spectroscopy reviews, 37 (4), 347 (2002); https://doi.org/10.1081/ASR-120016081

[11] Salmon Landi Jr., Iran Rocha Segundo, Elisabete Freitas, Mikhail Vasilevskiy, Joaquim Carneiro, Carlos José Tavares, Solid State Communications 341 (114573), 1 (2022); https://doi.org/10.1016/j.ssc.2021.114573

[12] Francis Tchomb Mabvuer, Fridolin Tchangnwa Nya, Guy Maurel Dzifack Kenfack, Solar Energy, 240, 193 (2020); https://doi.org/10.1016/j.solener.2022.05.037